

# Demonstration of a Linearized Traveling Wave Y-Fed Directional Coupler Modulator Based on Electro-Optic Polymer

Beom Suk Lee, Che-Yun Lin, Alan X. Wang, and Ray T. Chen, *Fellow, IEEE, Fellow, OSA*

**Abstract**—In this paper, we demonstrate a traveling wave linear modulator for high speed analog optical link applications. A two-section Y-fed directional coupler modulator based on electro-optic polymer is linearized with  $\Delta\beta$ -reversal technique to suppress the third-order intermodulation distortions. A traveling wave electrode with low RF loss and excellent velocity matching is designed and demonstrated with the bandwidth-length product of 125 GHz·cm. The 3-dB electrical bandwidth of 10 GHz and the spurious free dynamic range of  $110 \pm 3$  dB/Hz<sup>2/3</sup> over the modulation frequency of 2–8 GHz are measured from the fabricated device.

**Index Terms**—Directional coupler, electro-optic polymer, linear modulator, traveling wave electrode,  $\Delta\beta$ -reversal.

## I. INTRODUCTION

THE spurious free dynamic range (SFDR) of high frequency analog optical links is limited by the system noise (predominantly from the relative intensity noise of lasers and the shot noise of photodiodes) and the nonlinearity of the modulation process. There have been various efforts to improve the linearity of modulators either electronically [1], [2] or optically [3]–[5]. A common goal of these efforts is to lower the third-order intermodulation distortions (IMD3s) which appear when multiple tones of signals are carried over a link. A shortcoming common for all these linearization techniques is that the improved linearity is achieved at the expense of simple device design. A Y-fed directional coupler (YFDC) modulator, on the other hand, had been proven to possess a highly linear transfer function without loss of the simplicity of device design [6]. Even higher linearity is achievable when YFDC is incorporated with  $\Delta\beta$ -reversal technique [7], [8]. We previously demonstrated a two-section YFDC modulator with  $\Delta\beta$ -reversal at low modulation frequency as a proof of concept [9], where we achieved the SFDR of 119 dB/Hz<sup>2/3</sup> with 11 dB enhancement over the conventional Mach–Zehnder modulator.

Manuscript received February 03, 2011; revised April 20, 2011; accepted April 21, 2011. Date of publication May 05, 2011; date of current version June 13, 2011. This work was supported in part by the Defense Advanced Research Projects Agency (DARPA) under Contract W31P4Q-08-C-0160 monitored by Dr. Devnand Shenoy.

B. S. Lee, C.-Y. Lin, and R. T. Chen are with the University of Texas at Austin, Austin, TX 78758 USA (e-mail: bslee74@gmail.com; cheyunlin@gmail.com; raychen@uts.cc.utexas.edu).

A. X. Wang is with Omega Optics Inc., Austin, TX 78759 USA (e-mail: alan.wang@omegaoptics.com).

Color versions of one or more of the figures in this paper are available online at <http://ieeexplore.ieee.org>.

Digital Object Identifier 10.1109/JLT.2011.2150735

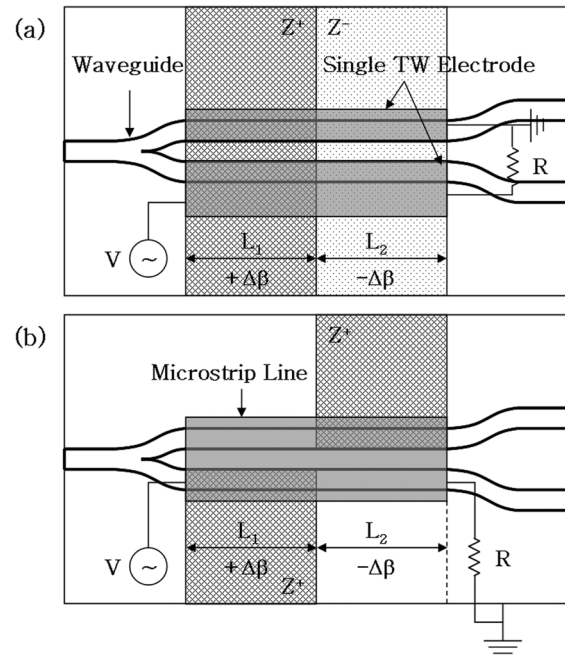


Fig. 1. Schematic layout of a traveling wave Y-fed directional coupler modulator with (a) true domain-inversion poling and (b) pseudo domain-inversion poling. ( $Z^+$ : poling direction is out of the surface,  $Z^-$ : poling direction is into the surface).

In this paper, we demonstrate a traveling wave YFDC modulator with  $\Delta\beta$ -reversal to extend our proven concept to GHz frequency regime. A traveling wave electrode with a unique design for RF microprobe coupling is fabricated with low RF loss and excellent velocity matching. The bandwidth-length product of 125 GHz·cm and the 3-dB electrical bandwidth of 10 GHz are achieved. The SFDR of  $110 \pm 3$  dB/Hz<sup>2/3</sup> is measured over the modulation frequency of 2–8 GHz.

## II. DESIGN OF A TWO-SECTION Y-FED DIRECTIONAL COUPLER MODULATOR WITH $\Delta\beta$ -REVERSAL

A YFDC shown in Fig. 1 has a single input waveguide that splits into two waveguides at proximity. Due to the symmetry of Y-splitter, equal optical power with the same phase is launched into the two waveguides and hence the device is automatically set at 3-dB operation point with zero bias. Proper design of coupling coefficient and interaction length can provide a linear transfer function [6]. The linearity of a YFDC modulator can be tailored to reduce IMD3 by introducing  $\Delta\beta$ -reversal technique [7], [8].  $\Delta\beta$ -reversal can be realized in the following way

in a two-section YFDC modulator. Directional coupler is divided into two sections and electro-optic (EO) polymer in the first section is poled in opposite direction with respect to the second section as noted  $Z^+$  and  $Z^-$  in Fig. 1(a) [10], which is called domain-inversion poling. An advantage of this configuration is that a single uniform traveling wave electrode can create  $\Delta\beta$ -reversal, which is desirable for high speed analog optical link applications. However, the domain-inversion poling requires pulsed poling technique to prevent dielectric breakdown at the boundary of the two adjacent poling electrodes with opposite polarity. Alternatively, pseudo domain-inversion poling is proposed in this paper as shown in Fig. 1(b). The lower- and upper waveguide respectively in the first- and second section is selectively poled in the same direction. Both waveguides of directional coupler are modulated by a single microstrip line but only one waveguide responds to the modulation field in each section due to the selective poling and hence the equivalent  $\Delta\beta$ -reversal effect can be achieved by normal poling process. An additional advantage of this configuration is that a uniform modulation field can be applied to both waveguides, which will be shown in the following section.

The linearity of a modulator is often characterized by distortion suppression which is defined as the ratio of fundamental signal to distortion signal. The distortion signal in this definition usually refers to IMD3 since IMD3 is the most troublesome among all distortions due to its proximity to fundamental signals. In a two-section YFDC modulator with  $\Delta\beta$ -reversal, IMD3 suppression is a sensitive function of the normalized interaction length ( $S_i$ ) which is defined as the ratio of the interaction length of  $i$ th section ( $L_i$ ) to the coupling length ( $L_c$ ) of directional coupler. Relative IMD3 suppression of a two-section YFDC modulator can be graphically represented by plotting the calculated IMD3 suppressions on ( $S_1, S_2$ ) plane [11].  $S_1 = S_2 = 2.86$  provides excellent linearity as well as very high modulation depth and is chosen for demonstration in this paper. The coupling length of directional coupler is matched to 3.5 mm by tuning the waveguide parameters and the corresponding total interaction length ( $L_1 + L_2$ ) is 2 cm.

### III. DESIGN OF A TRAVELING WAVE ELECTRODE

For high speed modulation at GHz frequency, it is essential to design a traveling wave electrode with the velocity matching between RF wave and optical wave as well as the characteristic impedance matching. Considering the alignment of modulation field with the direction of the  $r_{33}$  in poled EO polymer film, which is in vertical direction in our device configuration, a microstrip line is a natural choice for the best alignment. The characteristic impedance of a microstrip line is a function of the geometry parameters ( $w$ ,  $t$ , and  $h$  in Fig. 2(a)) and the relative dielectric constant ( $\epsilon_r$ ) of the substrate. The characteristic impedance can be expressed as [12]

$$Z_o = \frac{1}{c\sqrt{CC_o}} \quad (1)$$

where  $C$  is the capacitance per unit length,  $C_o$  is the capacitance per unit length of the structure when the substrate is replaced by

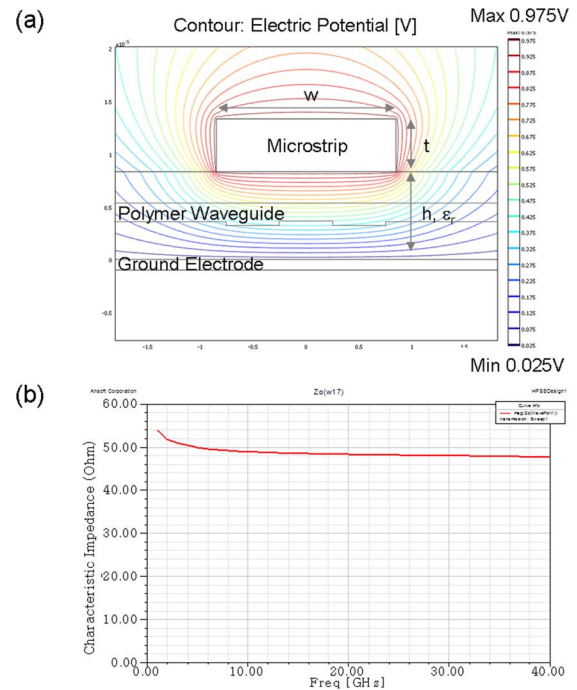


Fig. 2. (a) Schematic cross section of a microstrip line with design parameters (overlaid contour is the normalized electric potential calculated by COMSOL Multiphysics) (b) Frequency dependence of the characteristic impedance of a microstrip line calculated by Ansoft HFSS.

air, and  $c$  is the speed of light in air. COMSOL Multiphysics is employed to calculate the capacitance of our electrode structure. Given  $\epsilon_r = 3.2$ ,  $h = 8.3 \mu\text{m}$ , and  $t = 5 \mu\text{m}$  from the waveguide parameters and the fabrication conditions, the characteristic impedance of  $50 \Omega$  can be matched when  $w = 17$ . It can be seen in Fig. 2(a) that both waveguides are under the effect of a uniform modulation field between the microstrip and the ground electrode and hence the overlap integral between the optical mode and the modulation field can be maximized. Frequency dependence of the characteristic impedance is calculated with Ansoft HFSS based on the parameters given above. As shown in Fig. 2(b), the characteristic impedance varies within  $48\text{--}54 \Omega$  over the frequency range of  $1\text{--}40$  GHz.

To couple RF power from a RF microprobe into the microstrip line with minimum coupling loss, a tapered quasi-coplanar waveguide is designed as shown in Fig. 3(a) and (c). The width and gap of the coplanar waveguide ( $w$  and  $g$  in Fig. 3(c)) are gradually increased along the 1 mm long taper to match the dimension of a RF microprobe while maintaining the characteristic impedance at  $50 \Omega$ . Unlike the conventional coplanar waveguide, the bottom ground electrode under the taper is partially removed to suppress the formation of microstrip mode between the signal electrode and the bottom ground electrode. For this design to be valid, the resistivity of silicon substrate should be sufficiently high (typically  $\text{k}\Omega\text{-cm}$  or higher). Otherwise, the finite conductivity of silicon substrate allows the formation of microstrip mode between the signal electrode and silicon substrate. The microstrip mode would become dominant at wide part of the taper and hinder  $50 \Omega$  matching.

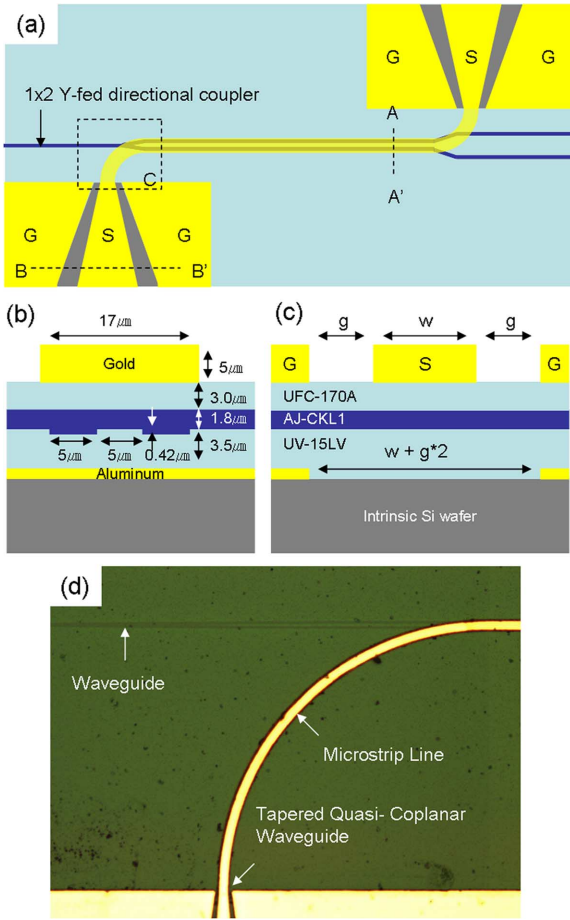


Fig. 3. (a) Schematic top view of electrode layout, (b) Schematic cross section corresponding to A–A' in (a), (c) Schematic cross section corresponding to B–B' in (a), and (d) Optical microscope image of the fabricated traveling wave electrode corresponding to C in (a). (S: signal electrode, G: ground electrode).

#### IV. FABRICATION

The device is fabricated on an intrinsic silicon wafer with 6–10 k $\Omega$ -cm resistivity. Polymer waveguide is fabricated on the prepatterned bottom electrode of 1  $\mu$ m aluminum film which serves as the ground electrode for poling process as well as for RF transmission. Polymer waveguide consists of three polymer layers (top: UFC-170A, core: AJ-CKL1, and bottom: UV-15LV). AJ-CKL1 (Dr. Alex Jen's research group, University of Washington) is formulated by doping 25 wt% of AJY chromophore into amorphous polycarbonate. Waveguide trench is patterned into the bottom cladding layer by photolithography and oxygen plasma reactive ion etching. Waveguide structure and parameters are presented in Fig. 3(b).

To create electro-optic effect in polymer waveguide, the device is poled by contact poling process. The electrode for pseudo domain-inversion poling is patterned by gold lift-off process. Peak poling temperature is 140°C, which is 5°C above the glass transition temperature of AJ-CKL1, and the applied poling electric field is 100 V/ $\mu$ m. The in-device  $r_{33}$  is measured to be 42 pm/V, which is 52.5% of the thin film  $r_{33}$  of AJ-CKL1.

The traveling wave electrode is fabricated by gold electroplating process. Seed layer of 50 nm gold with 5 nm chromium adhesion buffer is deposited by e-beam evaporation. Buffer

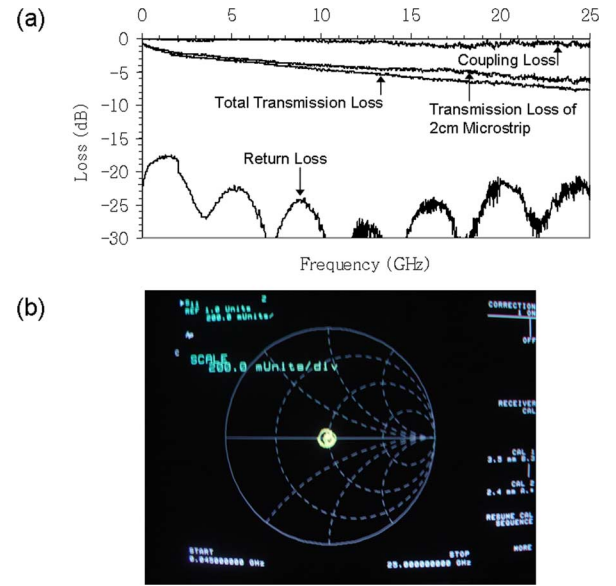


Fig. 4. (a) Loss of the fabricated traveling wave electrode, and (b) Characteristic impedance of the fabricated traveling wave electrode on Smith chart.

mask is patterned on 10  $\mu$ m AZ-9260 by photolithography. 5  $\mu$ m gold film is electroplated with Techni-Gold 25ES (Technic Inc.). The conductivity of the electroplated gold film is measured to be  $2.20 \times 10^7$  S/m. The coplanar- and bottom ground electrodes are connected with silver epoxy through a via-hole.

#### V. TESTING AND RESULTS

The performance of the fabricated traveling wave electrode is characterized by a vector network analyzer (HP 8510C). An air coplanar probe (ACP40-GSG-250, Cascade Microtech) is used to couple RF power into the tapered quasi-coplanar waveguide. RF loss of the fabricated traveling wave electrode is presented in Fig. 4(a). Return loss is well below  $-17$  dB. Square root frequency dependence of transmission loss implies that RF loss is dominated by conductor loss which is measured to be  $0.65 \pm 0.05$  dB/cm/GHz $^{1/2}$ . Low coupling loss is due to the excellent impedance matching of the tapered quasi-coplanar waveguide. It is shown in Fig. 4(b) that the characteristic impedance is well centered at 50  $\Omega$  on the Smith chart. The velocity matching between RF wave and optical wave is evaluated by the time domain measurement of the reflection loss. The effective relative dielectric constant of the microstrip line is measured to be 2.76 and the resulting index mismatch between RF wave and optical wave is 0.06. The bandwidth-length product due to the velocity mismatch can be expressed as [13]

$$(f \cdot L)_{\max} \cong \frac{c}{4|n_{\text{eff}} - \sqrt{\varepsilon_{\text{eff}}}|} \quad (2)$$

where  $f$  is the modulation frequency,  $L$  is the interaction length,  $c$  is the speed of light in air,  $n_{\text{eff}}$  is the effective refractive index of waveguide, and  $\varepsilon_{\text{eff}}$  is the effective relative dielectric constant of the microstrip line. The index mismatch of 0.06 results in the bandwidth-length product of 125 GHz-cm, so the modulation frequency limit corresponding to 2 cm interaction length would be 62.5 GHz.

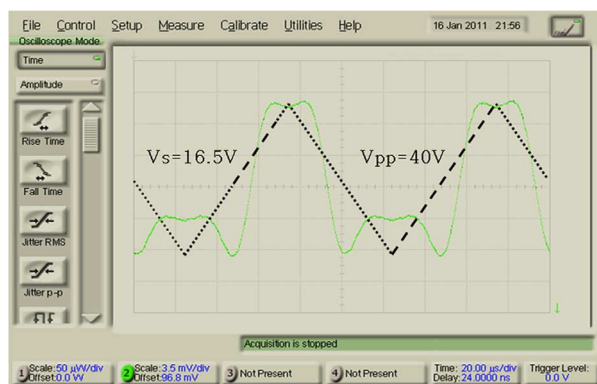


Fig. 5. Transfer function of over-modulation with  $V_{pp} = 40$  V at 10 kHz (wavelength =  $1.55 \mu\text{m}$ ).

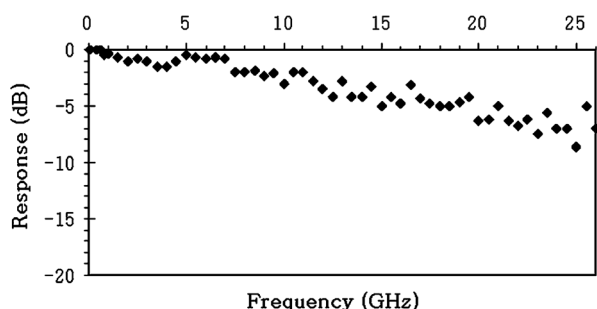


Fig. 6. Frequency response of the small signal modulation measured at 4% modulation depth.

The frequency response of the device is evaluated by the small signal optical modulation measured at 4% modulation depth. TM-polarized light with  $1.55 \mu\text{m}$  wavelength from a tunable laser (Santec ML-200, Santec Corp.) is launched into the input waveguide through a polarization maintaining fiber and the output light is collected by a single mode fiber. The measured optical insertion loss is 25 dB. The switching voltage measured by an over-modulation test is 16.5 V, which is much higher than our previous result (6.1 V in [9]) probably due to the lower poling efficiency of the selective poling process. Transfer function of the over-modulation test is shown in Fig. 5. For small signal optical modulation, RF signal from HP 83651B is fed into the traveling wave electrode through the RF microprobe. The modulated optical signal is boosted by an erbium doped fiber amplifier (Intelligain, Bay Spec Inc.), converted to electrical signal by a photodiode (DSC-R409, Discovery Semiconductors Inc.), and then measured by a microwave spectrum analyzer (HP 8560E). The measured 3-dB electrical bandwidth of the device is 10 GHz as shown in Fig. 6.

A two-tone test is performed to evaluate the linearity of the device. HP 8620C sweep oscillator is used as the second RF source for the two-tone input signals. Agilent 83020A and HP 8449B are used as pre- and post RF amplifier, respectively. The two input RF signals are combined by a coaxial two-way RF power combiner (RFLT2W1G04G, RF-Lambda). New Focus model-1014 is used for optical-to-electrical conversion of the modulated signal. The two-tone input signals and the resulting output signals are shown in Fig. 7(a) and (b), respectively. IMD3 signals, which are supposed to appear at one tone-interval

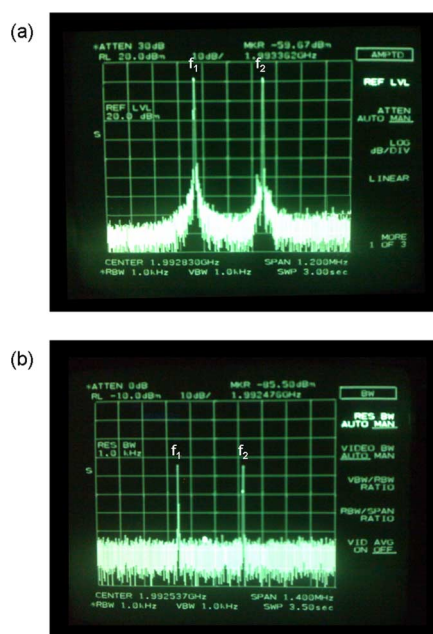


Fig. 7. (a) Input two-tone signals ( $f_1$  and  $f_2$ ) centered at 1.9928 GHz with 330 kHz tone-interval, and (b) Measured output fundamental signals.

away from the fundamental signals if present, are not observed in Fig. 7(b). A possible reason is that IMD3 signals are well suppressed and buried under the noise floor at this modulation depth. The power level of the two-tone input signals is 12 dBm as shown in Fig. 7(a), which is the maximum level available in our two-tone test setup, and this power level translates into the modulation depth of 15%. The simulation result in [14] predicts the IMD3 suppression at 15% modulation depth to be 74 dB and the corresponding experimental result in [9] is 69 dB, which is a reasonable value considering the fabrication and measurement errors. Neglecting the performance degradation due to RF loss and velocity mismatch, IMD3 signals would be 30 dB below the noise floor in Fig. 7(b) at 1 kHz bandwidth resolution.

Since the IMD3 suppression of the fabricated device is out of the measurable range in our two-tone test setup, SFDR is evaluated through an indirect method. It is known that, with the same modulation depth for both tones, IMD3 is three times or 9.54 dB higher than the third harmonic distortion [15]. The power level of mono-tone input signal is extended upto 29 dBm by combining the RF source (HP 83651B) with the pre-amplifier (Agilent 83020A). It is found that the third harmonic distortion of our device comes in the detectable range at the mono-tone input signal level above 20 dBm. IMD3 signals are obtained by adding 9.54 dB to the measured third harmonic distortion signals. SFDR is measured by extrapolating the IMD3 plot to find an intercept point with the noise floor, which is assumed at  $-160$  dBm considering the typical fiber-optic link parameters [16], and then measuring the difference with the extrapolated fundamental signal as illustrated in Fig. 8(a). The measured SFDR is within  $110 \pm 3$  dB/Hz $^{2/3}$  over the modulation frequency range of 2–8 GHz as shown in Fig. 8(b). The low end frequency is determined by the operation range (2–26.5 GHz) of the pre-amplifier (Agilent 83020A) and the high end is limited to 8 GHz because the third harmonic of the modulation frequency



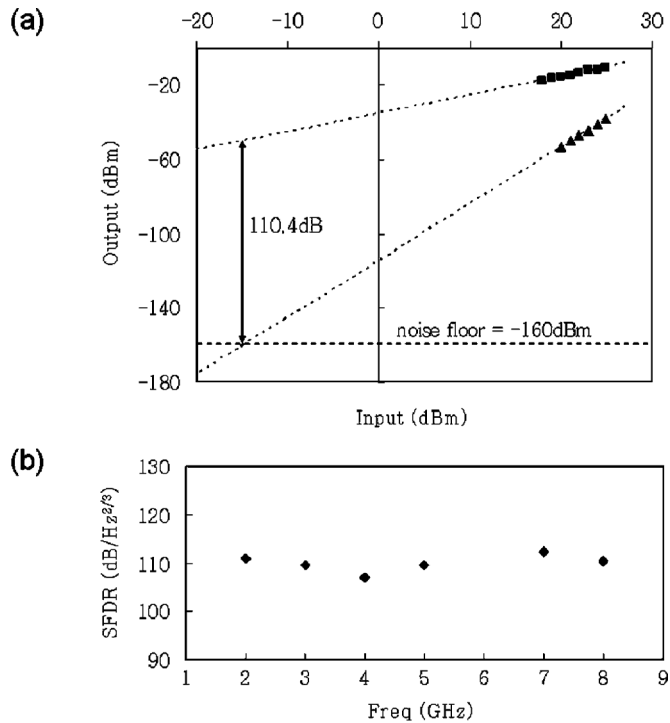


Fig. 8. (a) Plot of fundamental and third-order intermodulation distortion signals measured at 8 GHz, (b) Spurious free dynamic range measured at 2–8 GHz.

above 8 GHz goes beyond the scope ( $\sim 26.5$  GHz) of the microwave spectrum analyzer. The SFDR at 6 GHz is missing due to the irregular gain of the post-amplifier at 18 GHz. Schaffner *et al.* reported the SFDR of  $109.6 \text{ dB/Hz}^{2/3}$  at 1 GHz with a lithium niobate directional coupler modulator which is linearized by adding passive bias sections [17]. In their measurement, however, the noise floor was set at  $-171 \text{ dBm}$ , which offers  $7.3 \text{ dB}$  extra dynamic range compared with the noise floor at  $-160 \text{ dBm}$ . Hung *et al.* achieved even higher SFDR of  $115.5 \text{ dB/Hz}^{2/3}$  at 3 GHz with a linearized polymeric directional coupler modulator by subtracting the distortions of the measurement system [18]. Note that our SFDR of  $110 \pm 3 \text{ dB/Hz}^{2/3}$  includes the distortions from the entire measurement system as well as the device.

## VI. CONCLUSION

We have demonstrated a linearized traveling wave YFDC modulator based on EO polymer. Pseudo domain-inversion scheme is proposed and proven to provide the equivalent  $\Delta\beta$ -reversal effect as the domain-inversion poling of EO polymer. The traveling wave electrode is evaluated to be functional upto  $62.5 \text{ GHz}$  for our device design due to the excellent velocity matching between RF wave and optical wave. The SFDR of  $110 \pm 3 \text{ dB/Hz}^{2/3}$  is achieved over the modulation frequency of  $2\text{--}8 \text{ GHz}$ . The measured  $3\text{-dB}$  electrical bandwidth of the device is  $10 \text{ GHz}$ , which needs further improvement for practical applications.

## REFERENCES

[1] R. B. Childs and V. A. O'Byrne, "Predistortion linearization of directly modulated DFB lasers and external modulators for AM video transmission," in *Proc. Tech. Dig. Opt. Fiber Commun. Conf., OSA/IEEE*, San Francisco, CA, 1990, Paper WH6.

[2] R. M. DeRidder and S. K. Korotky, "Feedforward compensation of integrated-optic modulator distortion," in *Proc. Tech. Dig. Opt. Fiber Commun. Conf., OSA/IEEE*, San Francisco, CA, 1990, Paper WH5.

[3] L. M. Johnson and H. V. Rousell, "Reduction of intermodulation distortion in interferometric optical modulators," *Opt. Lett.*, vol. 13, no. 10, pp. 928–930, 1988.

[4] S. K. Korotky and R. M. Ridder, "Dual parallel modulation schemes for low-distortion analog optical transmission," *IEEE J. Sel. Areas Commun.*, vol. 8, no. 7, pp. 1377–1381, Jul. 1990.

[5] M. L. Farwell, Z.-Q. Lin, E. Wooten, and W. S. C. Chang, "An electrooptic intensity modulator with improved linearity," *IEEE Photon. Technol. Lett.*, vol. 3, no. 9, pp. 792–795, Sep. 1991.

[6] S. Thaniyavarn, "Modified  $1 \times 2$  directional coupler waveguide modulator," *Electron. Lett.*, vol. 22, no. 18, pp. 941–942, 1986.

[7] H. Kogelnik and R. V. Schmidt, "Switched directional couplers with alternating  $\Delta\beta$ ," *IEEE J. Quantum Electron.*, vol. QE-12, no. 7, pp. 396–401, Jul. 1976.

[8] R. F. Tavlykaev and R. V. Ramaswamy, "Highly linear Y-fed directional coupler modulator with low intermodulation distortion," *J. Lightw. Technol.*, vol. 17, no. 2, pp. 282–291, Feb. 1999.

[9] B. Lee, C. Lin, A. X. Wang, R. Dinu, and R. T. Chen, "Linearized electro-optic modulators based on a two-section Y-fed directional coupler," *Appl. Opt.*, vol. 49, no. 33, pp. 6485–6488, 2010.

[10] S. Tang, Z. Shi, D. An, L. Sun, and R. T. Chen, "Highly efficient linear waveguide modulator based on domain-inverted electro-optic polymers," *Opt. Eng.*, vol. 39, no. 3, pp. 680–688, 2000.

[11] B. Lee, C. Lin, X. Wang, R. T. Chen, J. Luo, and A. K. Y. Jen, "Bias-free electro-optic polymer-based two-section Y-branch waveguide modulator with  $22 \text{ dB}$  linearity enhancement," *Opt. Lett.*, vol. 34, no. 21, pp. 3277–3279, 2009.

[12] E. Yamashita, "Variational method for the analysis of microstrip-like transmission lines," *IEEE Trans. Microw. Theory Tech.*, vol. MTT-16, no. 8, pp. 529–535, Aug. 1968.

[13] A. Yariv, *Quantum Electronics*, 3rd ed. New York: Wiley, 1989, p. 322.

[14] X. Wang, B. Lee, C. Lin, D. An, and R. T. Chen, "Electrooptic polymer linear modulators based on multiple-domain Y-fed directional coupler," *J. Lightw. Technol.*, vol. 28, no. 11, pp. 1670–1675, 2010.

[15] P. Liu, B. J. Li, and Y. S. Trisno, "In search of a linear electrooptic amplitude modulator," *IEEE Photon. Technol. Lett.*, vol. 3, no. 2, pp. 144–146, Feb. 1991.

[16] W. B. Bridges and J. H. Schaffner, "Distortion in linearized electrooptic modulators," *IEEE Trans. Microw. Theory Tech.*, vol. 43, no. 9, pp. 2184–2197, Sep. 1995.

[17] J. H. Schaffner, J. F. Lam, C. J. Gaeta, G. L. Tangonan, R. L. Joyce, M. L. Farwell, and W. S. C. Chang, "Spur-free dynamic range measurements of a fiber optic link with traveling wave linearized directional coupler modulators," *IEEE Photon. Technol. Lett.*, vol. 6, no. 2, pp. 273–275, Feb. 1994.

[18] Y. Hung, S. Kim, H. , and Fetternam, "Experimental demonstration of a linearized polymeric directional coupler modulator," *IEEE Photon. Technol. Lett.*, vol. 9, no. 21, pp. 1762–1764, Dec. 2007.

**Beom Suk Lee** received the B.S. and M.S. degrees in material science and engineering from Seoul National University, Seoul, Korea, in 1999 and 2001, respectively. He is currently working toward the Ph.D. degree in electrical and computer engineering at the University of Texas at Austin.

His current research interests are all-polymeric and silicon-polymer hybrid optical modulators based on electrooptic polymer material.

**Che-Yun Lin** received the B.S. degree in electronic engineering from Chang Gung University, Taoyuan, Taiwan, in 2006, and the M.S.E. degree in electrical and systems engineering from the University of Pennsylvania, Philadelphia, in 2008. He is currently working toward the Ph.D. degree in the Department of Electrical and Computer Engineering, Microelectronics Research Center, University of Texas at Austin.

He is working with Prof. R. T. Chen's Optical Interconnect Group, where he is engaged in the design, fabrication, and characterization of RF photonic and silicon nano-photonics devices. His current research includes experimental demonstration of highly linear electrooptic modulator and silicon-organic hybrid photonic crystal waveguide modulator.

**Alan X. Wang** received the B.S. degree in material science and engineering from Tsinghua University, Beijing, China, in 2000, the M.S. degree in electrical engineering from the Chinese Academy of Sciences, Beijing, in 2003, and the Ph.D. degree in electrical engineering from the University of Texas at Austin in 2006. His Ph.D. research work included polymer optical switches, photonic devices for phased array antennas, and board level optical interconnects.

He is currently a Research Scientist with Omega Optics Inc., Austin, TX, where his research focuses on nano-photonics, RF photonics, optical interconnects, and optical sensing.

**Ray T. Chen** (F'04) received the B.S. degree in physics from National Tsing-Hua University, Hsinchu, Taiwan, in 1980 and the M.S. degree in physics and the Ph.D. degree in electrical engineering from the University of California in 1983 and 1988, respectively.

He holds the Cullen Trust for Higher Education Endowed Professorship at the University of Texas at Austin (UT Austin). He joined UT Austin as a member of faculty to start optical interconnect research program in the Electrical and Computer Engineering Department in 1992. Prior to his professorship with UT Austin, he was a Research Scientist, Manager, and Director of the Department of Electrooptic Engineering, Physical Optics Corporation, Torrance, CA, from 1988 to 1992. He also served as the CTO/founder and chairman of the board of Radiant Research from 2000 to 2001, where he raised \$18 million. A-Round funding to commercialize polymer-based photonic devices. He has also served

as the founder and Chairman of the board of Omega Optics Inc., Austin, TX, since its initiation in 2001. His research work has been awarded with 84 research grants and contracts from such sponsors as the Department of Defense, the National Science Foundation, the Department of Energy, NASA, the State of Texas, and private industry. The research topics are focused on three main subjects: nano-photonics passive and active devices for optical interconnect applications, polymer-based guided-wave optical interconnection and packaging, and true time delay (TTD) wideband phased-array antenna (PAA). Experiences garnered through these programs in polymeric material processing and device integration are pivotal elements for the research work conducted by his group. His group at UT Austin has reported its research findings in more than 420 published papers including over 55 invited papers. He holds 12 issued patents. He has served as an editor or co-editor for 18 conference proceedings. He has also served as a consultant for various federal agencies and private companies and delivered numerous invited talks to professional societies.

Dr. Chen is a Fellow of the Optical Society of America (OSA) and The International Society of Optical Engineering (SPIE). He has chaired or been a program-committee member for more than 50 domestic and international conferences organized by IEEE, SPIE, OSA, and PSC. He was the 1987 recipient of UC Regent's dissertation fellowship and of the UT Engineering Foundation Faculty Award in 1999 for his contributions in research, teaching and services. Back to his undergraduate years in National Tsing-Hua University, he led a university debate team in 1979 which received the national championship of national debate contest in Taiwan. There are 33 students received the E.E. Ph.D. degree in his research group at UT Austin.